Acta Med. Okayama, 2007
Vol. 61, No. 2, pp. 63–69

Acta Medica Okayama
http://www.lib.okayama-u.ac.jp/www/acta/

Original Article

Resolution of Pulmonary Multiplanar Reconstruction Images from 0.5-mm Theoretical Isotropic Data: A Fundamental Study Using an Inflated and Fixed Lung Specimen

Daisuke Maki[a]*, Masashi Takahashi[b], Noritoshi Ushio[b], Ryutaro Takazakura[b], Norihisa Nitta[b], Kiyoshi Murata[b], and Susumu Kanazawa[a]

[a]Department of Radiology, Okayama University Graduate School of Medicine, Dentistry and Pharmaceutical Sciences, Okayama 700–8558, Japan, and
[b]Department of Radiology, Shiga University of Medical Science, Otsu, Shiga 520–2192, Japan

The aim of the present study was to define the resolution of multiplanar reconstruction (MPR) of the lung from "theoretical isotropic data." Using inflated and fixed lung specimens of the pig placed in the chest wall phantom, 0.5-mm isotropic data were obtained with 2 different helical pitches: 1:7 (high-quality mode) or 1:13, (high-speed mode), and 2 different tube currents: 250 mAs (high-tube-current mode) or 100 mAs (low-tube-current mode), with or without overlapping reconstruction. MPRs were created from these axial data. The diameter of the smallest visible pulmonary artery and bronchi of these CT images were measured on the corresponding slices of the specimen. The high-speed and low-tube-current mode significantly degraded the image quality due to increased noise. The smallest visible pulmonary artery and bronchus resolved on MPRs from axial-spiral data with 0.5-mm collimation were approximately 100 μm and 1,000 μm in diameter, respectively. In conclusion, helical pitch and tube current influence the resolution of MPR of the lung.

Key words: multiplanar reconstruction, computed tomography, lung

The usefulness of multiplanar reconstruction (MPR) has been reported in a variable imaging field and application to the chest, including the diagnosis of diaphragmatic trauma [1, 2], volumetric expiratory scan [3], and diffuse lung disease [4, 5] has been attempted. Remy-Jardin *et al.* have reported that coronal MPR images from 1.0-mm collimation allow a diagnostic approach to diffuse lung disease as precise as that provided with axial high resolution CT (HRCT) scans and reduce the number of images compared with axial images [4]. The other expected benefit of coronal HRCT is an easy analysis of cranio-caudal extension of the diffuse lung disease, which is critical in making a differential diagnosis [5]. Comparison in the same direction as the chest x-ray is beneficial. A stair-step artifact appearing as a stripe on the MPR image is a problem of MPR images and collimation, and the table feed significantly affects its severity [6]. The stair-step artifact can be improved by overlapping reconstructions of axial data [6, 7]. The concept of "isotropic voxel" was first proposed in 1995 [8]. Isotropic data theo-

Received August 15, 2006; accepted November 24, 2006.
*Corresponding author. Phone:+81–86–235–7313; Fax:+81–86–235–7316
E-mail:daimaki525@ybb.ne.jp (D. Maki)

retically promise image reconstruction in any arbitrary direction with preservation of spatial resolution. The advantage of this concept is enhanced by the development of multi-detector CT (MDCT) technology. MDCT has the ability to cover a long z-axis with a thinner section, as well as a shorter scan time [9]. Honda *et al.* have reported that when using inflated and fixed lung specimen, the image quality of coronal MPR from isotropic voxel data obtained using 0.5-mm collimation, with or without overlapping reconstruction, is similar to that of direct coronal thin-section CT scans [10]. Correct recognition of normal lung structure is indispensable to diagnosing diffuse lung disease not only on HRCT but also on high-resolution MPR [11]. The resolutions on the MPR image of the normal lung structure and the influence of helical pitch and tube current with a chest wall phantom have not been reported. Helical pitch and tube current influence the quality of CT imaging. High helical pitch reduces the scan time and radiation exposure but degrades the quality of CT imaging [12]. The purposes of this study are: 1) to evaluate how helical pitch and radiation dose influence the resolution of MPR images, and 2) to evaluate how MPR images from axial spiral data with 0.5-mm collimation precisely show normal lung structure.

Materials and Methods

Preparation of specimen. A pig lung without any pulmonary disorders was used (cross-species of Yorkshire, Landrace and Barkshire, weight 30 kg), because the structure of pig lung is similar to that of the human lung, especially at the level of the secondary pulmonary lobule. Warm 15% gelatin was injected into the pulmonary arteries at a pressure of 25 cm H_2O until the solution came back from the pulmonary vein. The CT attenuation of the solution was approximately 30 HU, which is similar to that of blood [11]. The lungs were distended and fixed by the method of Markarian and Dailey [13]. They were distended through the main bronchus with a fixative fluid containing polyethylene glycol 400, 95% ethyl alcohol, 40% formalin, and plain water in a proportion of 10:5:2:3 and immersed in the fixative for 2 days. The fixed lung was then air-dried. Four blocks ($4 \times 4 \times 1$ cm, $4.5 \times 3 \times 1$ cm, $6 \times 4.5 \times 1.5$ cm, $6 \times 5.5 \times 2$ cm) were excised from the specimen to be cut on a microslicer (DTK 1000 W, Dosaka EM, Kyoto, Japan).

CT protocol. The pig lung specimen was placed in the originally developed chest wall phantom (Taisei Medical, Osaka, Japan). This phantom was manufactured to simulate the specimen within the human thoracic cage (Fig. 1). The simulated spine and ribs were embedded in a soft tissue density material. The soft tissue part of the phantom (specific gravity: 1.03) was made of polyurethane, and the bone of the phantom (specific gravity: 1.45) was made of calcium carbonate, paraffin, polyethylene, rosin, titanium-dioxide, and magnesium-dioxide. The specimen slices were scanned using 8-multidetector CT (Aquillion: Toshiba, Tokyo, Japan). Axial images were obtained with the following technical factors: 1) high-quality mode with high-tube-current mode or low-tube-current mode: 0.5-mm collimation, 0.5-mm reconstruction interval or 0.3-mm reconstruction (overlapping) with high-quality mode (helical pitch 7) with high-tube-current mode (250 mAs) or low-tube-current mode (100 mAs), and 2) high-speed mode with high-tube-current mode or low-tube-current mode: 0.5-mm collimation, 0.5-mm reconstruction interval or 0.3-mm reconstruction (overlapping) with high-speed mode (helical pitch 13) with high-tube-cur-

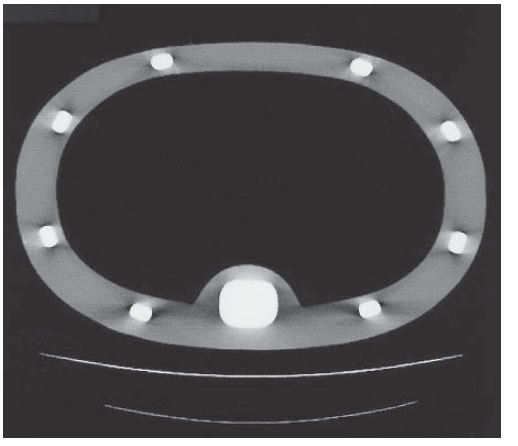

Fig. 1 — Chest wall phantom: The soft tissue portion of the phantom (specific gravity: 1.03) was made of polyurethane, and the bone of the phantom (specific gravity: 1.45) was made of calcium carbonate, paraffin, polyethylene, rosin, titanium-dioxide, and magnesium-dioxide.

rent mode (250 mAs) or low-tube-current mode (100 mAs). All scans were obtained using 0.5 sec per rotation, 120 kV, 25.6 cm field of view, 512 × 512 matrix, and a high-frequency reconstruction algorithm. (Table 1).

Contact radiograph of the specimen. Four blocks of the specimen were cut into contiguous 0.5-mm thick slices at precisely the same planes as those of the CT images using the microslicer. The contact radiographs of these slices were obtained with a fine-grain film (X-OMAT-TL film, Eastman-Kodak, Rochester, NY, USA) at 15 kVp, 90 mAs, and 60 cm tube-film distance.

Evaluation of the smallest visible pulmonary artery and bronchus. The smallest visible pulmonary arteries were identified on CT images. They were defined as the last ordered branching structure of the pulmonary artery clearly resolved on the CT images. The continuity of the vessel structure from the hilar to the peripheral side in the serial slices and the acknowledgement of the accompanying bronchus were helpful when the observers had difficulty in identifying pulmonary artery. To guarantee the objectivity of the procedure, the following steps were employed. One board-certified chest radiologist (D.M.) defined the smallest visible artery on CT images and marked the corresponding points on the contact radiograph. Another board-certified chest radiologist (M.T.) then confirmed these findings, and the diameter of the pulmonary artery was measured using a stereomicroscope. When a discrepancy occurred, the images were reviewed until consensus was reached. The outer diameter and wall thickness of the smallest visible bronchus were also measured.

In the study, these data were compared with changing helical pitch, the reconstruction interval, as well as the tube current.

Statistics. Statistical analysis was performed using Mann-Whitney's U-test with commercially available software (StatView 5.0; SAS Institute Inc, Cary, NC, USA). P values less than 0.05 were regarded as statistically significant.

Table 1 The CT protocols

Collimation-reconstruction interval	Helical pitch	Tube current (mAs)
0.5 mm–0.5 mm	7	250
0.5 mm–0.3 mm	7	250
0.5 mm–0.5 mm	7	100
0.5 mm–0.3 mm	7	100
0.5 mm–0.5 mm	13	250
0.5 mm–0.3 mm	13	250
0.5 mm–0.5 mm	13	100
0.5 mm–0.3 mm	13	100

Results

MPR images with high-quality mode (HP 7): high-tube-current mode (250 mAs) versus low-tube-current mode (100 mAs). The frequency distribution of the outer diameter of the smallest visible pulmonary arteries and bronchi in the peripheral lung are shown in Fig. 2. There was no difference in the distributions between the MPR images with and without overlapping reconstructions both in high and low-tube-current mode, and it is considered that the resolution of both MPR images was equivalent (Figs. 2, 3). The smallest visible pulmonary artery and bronchus resolved on MPR images with high-quality mode with high-tube-current mode were approximately 100 μm and 1,000 μm (wall thickness 100 μm) in diameter, respectively (Fig. 2). No statistically significant difference was found between the resolution of pulmonary arteries on MPR images with high and low-tube-current mode ($p = 0.085$). The resolution of bronchus on the low-tube-current mode was significantly less than that of the high-tube-current mode ($p = 0.006$). Although the greater amount of noise and the vagueness of small lung structures were more significant on the low-tube-current mode than on the high-tube-current mode, small lung structures such as pulmonary arteries 100 μm in diameter or bronchi 1,000 μm in diameter still could be resolved on the low-tube-current mode (Figs. 2, 3).

MPR images with high-speed mode (HP 13): high-tube-current mode (250 mAs) versus low-tube-current mode (100 mAs). The frequency distribution of the outer diameter of the smallest visible pulmonary arteries and bronchi in the peripheral lung are shown in Fig. 4. There was no difference in the distributions between the MPR images with and without overlapping reconstructions

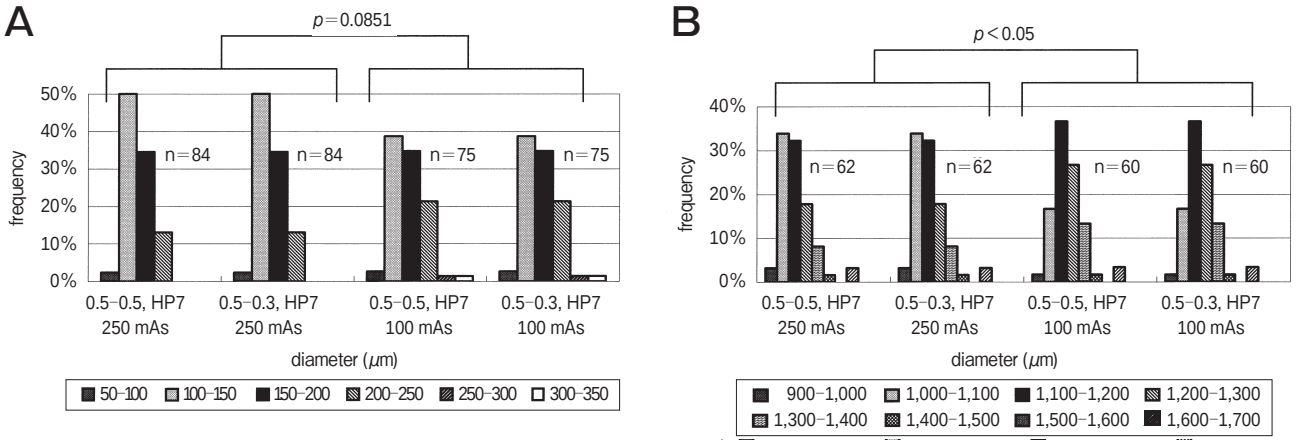

Fig. 2 The frequency distribution of the outer diameter of the smallest visible pulmonary artery **A** and bronchus **B** with high-quality mode (pitch 7) with high-tube-current mode (250 mAs) or low-tube-current-mode (100 mAs): % = distribution of the smallest visible pulmonary artery and bronchus in the peripheral lung, 0.5-0.5, HP7 or 0.5–0.3, HP7 = 0.5-mm collimation, 0.5 or 0.3-mm reconstruction and helical pitch 7. MPR images with the high-quality mode can resolve the pulmonary artery under 100 μm in diameter and bronchi under 1,000 μm in diameter, even with low-tube-current mode. The resolution of each MPR protocol with overlapping reconstruction is equal to that of each MPR protocol without overlapping reconstruction.

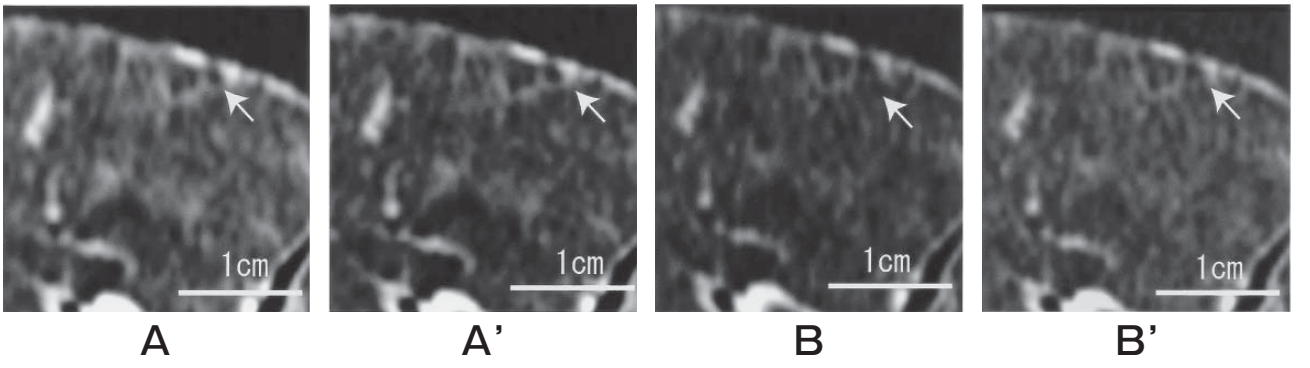

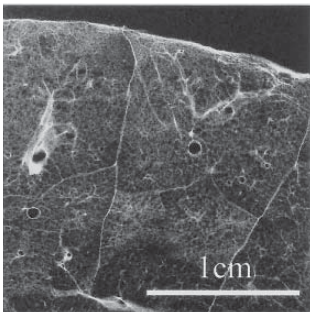

Fig. 3 MPR images with high-quality mode with high-tube-current or low-tube-current mode: **A**, MPR image with 0.5-mm collimation, 0.5-mm reconstruction interval, high-quality mode and high-tube current mode: 250 mAs; **A'**, MPR image with 0.5-mm collimation, 0.3-mm reconstruction interval, high-quality mode, and high-tube current mode; **B**, MPR image with 0.5-mm collimation, 0.5-mm reconstruction interval, high-quality mode, and low-tube-current mode: 100 mAs; **B'**, MPR image with 0.5-mm collimation, 0.3-mm reconstruction interval, high-quality mode, and low-tube-current mode; **C**, contact radiograph Although with high-quality mode, the noise and vagueness of lung structures are more significant with low-tube-current mode than high-tube-current mode, small lung structures are still resolved on the former (white arrow).

in both high and low-tube-current mode, and it is considered that the resolution of both MPR images was equivalent (Figs. 4, 5). With high-speed mode, the resolution of MPR images with low-tube-current mode was significantly less than that of MPR images with high-tube-current mode (artery: $p = 0.033$, bronchus: $p = 0.009$). Noise and vagueness of lung structures were prominent on MPR images with high-speed-mode with low-tube-current mode. Some of the pulmonary arteries under 200 μm in diameter and bronchi under 1,500 μm could not be resolved (Figs. 4, 5).

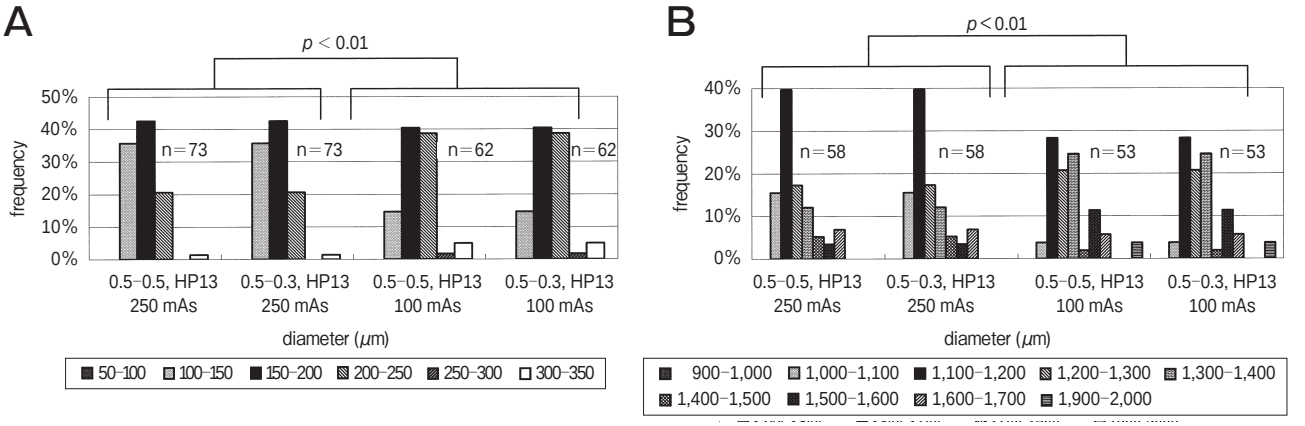

Fig. 4 The frequency distribution of the outer diameter of the smallest visible pulmonary artery **A** and bronchus **B** with high-speed mode (pitch 13) with high-tube-current mode (250 mAs) or low-tube-current-mode (100 mAs): % = distribution of the smallest visible pulmonary artery and bronchus in the peripheral lung, 0.5-0.5, HP13 or 0.5–0.3, HP13 = 0.5-mm collimation, 0.5 or 0.3-mm reconstruction and helical pitch 13. MPR images with high-speed mode cannot resolve pulmonary artery under 100 μm in diameter and bronchi under 1,000 μm in diameter, especially with low-tube-current mode. The resolution of each MPR protocol with overlapping reconstruction is equal to that of each MPR protocol without overlapping reconstruction.

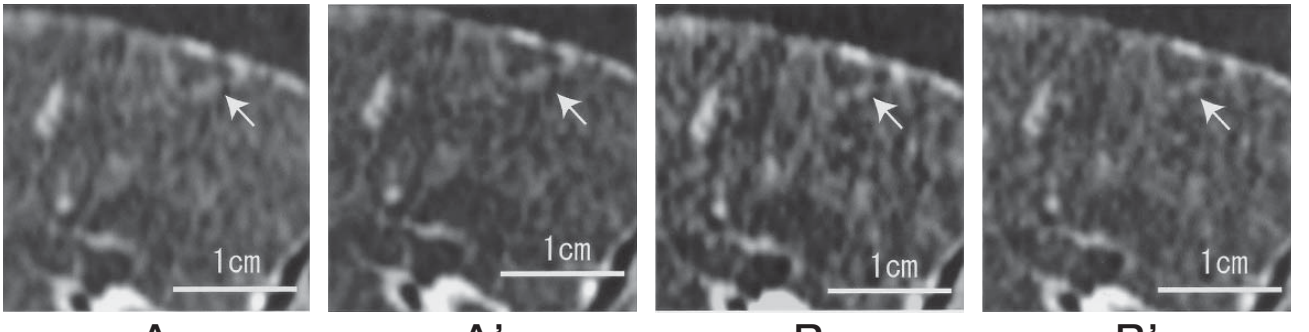

Fig. 5 MPR images with high-speed mode with high-tube-current or low-tube-current mode: **A**, MPR image with 0.5-mm collimation, 0.5-mm reconstruction interval, high-speed mode, and high-tube-current mode: 250 mAs; **A'**, MPR image with 0.5-mm collimation, 0.3-mm reconstruction interval, high-speed mode, and high-tube-current mode; **B**, MPR image with 0.5-mm collimation, 0.5-mm reconstruction interval, high-speed mode, and low-tube-current mode: 100 mAs; **B'**, MPR image with 0.5-mm collimation, 0.3-mm reconstruction interval, high-speed mode, and low-tube-current mode. Noises and vagueness of the lung structures are prominent on MPR images with high-speed mode. Especially with low-tube current mode, noise is confusing with small lung structures (white arrow). These types of noise are confusing with both small lung structures and pathologic lesions.

Discussion

The CT protocols were theoretically designed to obtain 0.5-mm isotropic data by using 0.5-mm collimation, a 25.6-cm field of view, and a 512×512 matrix. MPR images from isotropic data theoretically do not require overlapping reconstruction to improve the image quality. Honda *et al.* [10] have reported that the image quality of MPRs from isotropic data is similar to that of direct coronal scans and that overlapping reconstruction is not needed to improve the image quality of those MPRs when the human lung specimen was scanned by a 4-detector MDCT with a pitch of 6:1. Although it is speculated that the resolution of MPR images with a higher pitch, more than 13:1, might be improved by using overlapping reconstruction, a higher pitch mode could not be selected due to the limitation of the installed CT program in our machine.

Previous studies evaluating MPR images or HRCT have primarily been performed by comparison with direct CT scans of lung specimens [10, 11]. However, it is important to determine the deterioration effect by the thoracic cage and the influence of the tube current on the image quality of MPR from a clinical perspective. In this study, the influence of the tube current was determined by using an originally developed chest wall phantom. The phantom was designed to simulate a scan within the human chest wall and theoretically induces the beam-hardening artifacts from the spine and ribs.

The results show that helical pitch and the tube current significantly influence the visibility of peripheral vessels and bronchi on MPR. The reasons are considered due to the increasing beam-hardening artifact and the decreased resolution along the z-axis. It was speculated that MPR with high pitch and low tube current scan should not be used in evaluating detailed changes occurring in the lung field.

In our study, on MPR images with 0.5-mm collimation, a pitch of 7, and 250 mAs, the resolution of pulmonary arteries was 100 μm in diameter, and that of bronchi was 1,000 μm in diameter. In human lung, pulmonary arteries 100 μm in diameter are theoretically within 1 mm of the pleura [14]. Bronchi 1,000 μm in diameter are found 1–2 cm from the pleura and correspond to the level of bronchi approaching the secondary lobule of Reid [15–17]. In 1986, Murata *et al.* [11] have reported that on 1.5-mm collimation HRCT, the resolution of pulmonary arteries is 200 μm in diameter and that of bronchi is 2 mm. Later, on 0.5-mm collimation HRCT, Takahashi *et al.* reported a pulmonary artery resolution of 100 μm and a bronchial resolution of 400 μm [13]. MPR images with high-quality mode and 0.5-mm isotropic data successfully demonstrate the peripheral lung structures, even in the secondary pulmonary lobule. These results suggest that high-resolution MPR can be used in the evaluation of diffuse lung disease.

This study had several limitations. First, the determination of the smallest visible pulmonary artery and bronchus was not objective. Although the consistency of these determinations was confirmed between 2 radiologists, it was not possible to guarantee complete objectivity. Second, a motion artifact cannot be evaluated using a lung specimen. A motion artifact would probably worsen the stair-step artifact of MPR, especially with a high-pitch scan. Third, this study could not quantify the grade of noise or distortion of the visible lung structures since the criteria used was either "visible" or "invisible." Fourth, there was space between the lung specimen and a chest wall phantom and there was a possibility of influencing the appearance of the beam-hardening artifact.

In conclusion, helical pitch and radiation dose influence the resolution of MPR images due to increased noise. Overlapping reconstructions are not needed to improve the resolution of MPR images with 0.5-mm collimation. MPR images can demonstrate the peripheral lung structures, even in the secondary pulmonary lobule.

References

1. Israel RS, McDaniel PA, Primack SL, Salmon CJ, Fountain RL and Koslin DB: Diagnosis of diaphragmatic trauma with helical CT in a swine model. Am J Roentgenol (1996) 167: 637–641.
2. Larici AR, Gotway MB, Litt HI, Reddy GP, Webb WR, Gotway CA, Dawn SK, Marder SR and Storto ML: Helical CT with sagittal and coronal reconstructions: Accuracy for detector of diaphragmatic injury. Am J Roentgenol (2002) 179: 451–457.
3. Nishino M, Kuroki M, Boiselle PM, Copeland JF, Raptopoulos V and Hatabu H: Coronal reformations of volumetric expiratory high-resolution CT of the lung. Am J Roentgenol (2004) 182: 979–982.
4. Remy-Jardin M, Campistron P, Amara A, Mastora I, Tillie-Leblond I, Delannoy V, Duhamel A and Remy J: Usefulness of

coronal reformations in the diagnostic evaluation of infiltrative lung disease. J Comput Assist Tomogr (2003) 27: 266–273.
5. Arakawa H, Sasaka K, Lu WM, Hirayanagi N and Nakajima Y: Comparison of axial high-resolution CT and thin-section multiplanar reformation (MPR) for diagnosis of disease of the pulmonary parenchyma: Preliminary study in 49 patients. J thorac Imaging (2004) 19: 24–31.
6. Wang G and Vannier MW: Stair-step artifact in three-dimensional helical CT: An experimental study. Radiology (1994) 191: 79–83.
7. Kasales CJ, Hopper KD, Ariola DN, TenHave TR, Meilstrup JW, Mahraj RPM, Van Hook D, Westacott S, Sefczek RJ and Barr JD: Reconstructed helical CT scans: Improvement in z-axis resolution compared with overlapping and nonoverlapped conventional CT scans. Am J Roentgenol (1995) 164: 1281–1284.
8. Kalender WA: Thin-section three-dimensional spiral CT: Is isotropic imaging possible? Radiology (1995) 197: 578–580.
9. Hu H: Multi-slice helical CT: Scans and reconstruction. Med Phys (1999) 26: 5–18.
10. Honda O, Johkoh T, Yamamoto S, Koyama M, Tomiyama N, Kozuka T, Hamada S, Mihara N, Nakamura H and Muller NL: Comparison of quality of multiplanar reconstructions and direct coronal multidetector CT scans of the lung. Am J Roentgenol (2002) 179: 875–879.
11. Murata K, Itoh H, Todo G, Kanaoka M, Noma S, Itoh T, Furuta M, Asamoto H and Torizuka K: Centrilobular lesion of the lung: Demonstration by high-resolution CT and pathologic correlation. Radiology (1986) 161: 641–645.
12. Honda O, Johkoh T, Tomiyama N, Kozuka T, Mihara N, Koyama M, Hamada S, Naito H, Nakamura H and Kudo M: High-resolution CT using multidetector CT equipment: evaluation of image quality in 11 cadaveric lungs and a phantom. Am J Roentgenol (2001) 177: 875–879.
13. Markarian B and Dailey ET: Preparation of inflated lung specimens; in The lung: radiologic-pathologic correlations, Heitzman ER ed, 3 rd Ed, Mosby, St. Louis (1993) pp 4–12.
14. Takahashi M, Nitta N, Takazakura R, Nishimoto Y and Murata K: 0.5 mm thickness HRCT: How precisely are the normal and abnormal lung structures demonstrated? Part 1: fundamental study using inflated and fixed lung specimen. Radiology (2002) 225 (p) (abstract): 144–145.
15. Takahashi M, Nitta N, Takazakura R, Nishimoto Y and Murata K: 0.5 mm thickness HRCT: how precisely are the normal and abnormal lung structures demonstrated? Part 2: normal volunteers and clinical studies. Radiology (2002) 225 (p) (abstract): 145.
16. Reid L and Simon G: The peripheral pattern in the normal bronchogram and its relation to peripheral pulmonary anatomy. Thorax (1958) 13: 103–109.
17. Reid L: The secondary lobule in the adult human lung, with special reference to its appearance in bronchograms. Thorax (1958) 13: 110–114.